

## 3 Sky Pattern of Space Debris Detectability (“SkyPlot”) - Introduction

### 3.1 Introduction

This chapter is concerned with the detectability of space debris, specifically, the combined effect that time-varying illumination and variable background brightness characteristics have on the altitude-azimuth (“alt-az”) pattern (a “sky plot”) in the observer’s sky, and seeks to characterise any patterns that arise due to these effects. The reason for doing this is twofold:

1. Does the detection rate vary as a function of telescope pointing direction?
2. If so, try to identify “hot spots” where detection rates could be optimised for given scenarios of orbit/site/observation period.

A skyplot in this sense is a contour map of the sky at a given site divided into  $2^\circ \times 2^\circ$  alt-az bins, each representing the total time that a particular debris fragment is detectable ( $\text{SNR} \geq 3$ ) in a  $1^\circ \times 1^\circ$  telescope field of view (FOV) for the observation period specified. Thus a “hot spot” in the skyplot denotes an area for which the debris is more visible during the simulated period, while a “cold spot” depicts a part of the sky where debris is rarely or never seen over the same period.

Considering a given telescope/detector system at a given geographical site, the optical SNR of space debris in a particular orbit will be influenced by many factors, which may be put into two broad groups (Table 3-1):

All of these factors conspire to produce complex skyplots that are non-intuitive to predict, and are difficult to calculate analytically. For any orbit other than of low eccentricity, analytical models are of limited utility and numerical analysis is the preferred method (Larson & Wertz, 1992).

The purpose of this investigation is to determine the observability of a particular orbit, not that of a particular debris particle. In this way the optimum conditions of observing an orbit under varying background/lighting conditions can be investigated (a standard orbital evolution model would propagate the debris particle over time out of the original orbit into a different orbit). This is achieved by populating the orbit with a large number of particles and averaging the results (see chapter 5).

Factors inherent to debris	External factors
Debris size Debris shape Debris albedo Sun-Debris-Observer phase angle Topocentric angular speed	Weather at observing site Earth Shadowing Brightness of twilight sky Brightness of moonlit sky Brightness of light-polluted sky Milky Way background Zodiacal Light background Atmospheric extinction

Table 3-1: Broad grouping of factors determining apparent debris particle brightness.

## 3.2 Code Structure

At the time the SkyPlot code was devised (1993-4), the only affordable satellite simulation programs available that gave some results on the optical visibility of Earth satellites were STSPLUS and PC-TRACK. Both were shareware and provided means to determine the position of satellites in the observer's sky, but did not provide the means to perform any analysis of the quality of the observation other than saying the satellite was/was not illuminated by the Sun. The orbital model STSPLUS employed was valid only for near-circular LEO satellites. PC-TRACK fared better in that the orbit types it could handle were not as restrictive, i.e. the full range from LEO to GSO, but again the quality of the data was just stating if the debris was visible, with no indication of brightness. In both cases, the source code was not available for modification.

## 3.3 Program Execution - Overview

The SkyPlot program is a numerical rather than an analytical program. Analytical treatments are possible for satellites in circular orbits because of the simplicity of the case. However as this program also deals with highly eccentric orbits, the situation is more complex; such are best solved by numerical methods (Larson & Wertz, 1992).

Inputs to the program are:

- Site latitude, longitude, height above sea level
- Telescope operating parameters (optics, detector, integration time etc)
- Debris orbital elements, physical characteristics.
- Start and finish dates. The interval between these dates is referred to as the "observing run".

The program then executes in the following manner: The annual astronomical twilight environment for sites with latitudes greater than  $\pm 48.2^\circ$  is determined, i.e. such sites will experience a sky brightness greater than that of astronomical twilight\* lasting all night during local summer. The program determines the dates at which this effect begins and ends and avoids that twilight “window” during execution, should it overlap with the observing run.

Abort Scenarios: Based on the inputs and calculated twilight environment, any scenario or combination of parameters that would cause debris never to be detected by the observer is assessed. If such is the case the program aborts immediately with an appropriate diagnostic message.

The program then begins by incrementing the time by a pre-set amount (referred to as a “timestep”), starting from the onset of astronomical twilight on the evening of the first day. For each timestep the position vectors of the observer and debris are calculated and from these the position of the debris in the observer’s sky is determined. If the debris meets criteria for being visible (above horizon, out of Earth shadow, Moon below horizon) it is flagged as visible and further details are calculated: the azimuth; signal to noise ratio (taking into account background sky and detector noise sources); and topocentric angular velocity. These details are binned in a multi-dimensional results array such that each bin is incremented by one timestep value.

At the onset of dawn twilight the program jumps to evening twilight for the next night, while incrementing the position of the Sun and Moon and performing orbit evolution, and the program continues as before. This aspect of the program’s structure was introduced to cut execution time. With the rapid increase in computing speed in recent years this technique is not as important as it used to be.

The program continues in this fashion, incrementing bins as appropriate whenever the debris is visible, until the date reaches that of the end of the observing run. At this point, the results array is open for interrogation.

A detailed flowchart showing the salient points of the above description, plus some other points of interest covered in chapter 4, is shown in Figure 3.1.

---

\* Defined as the brightness of the night sky when the Sun is at least  $18^\circ$  below the horizon.

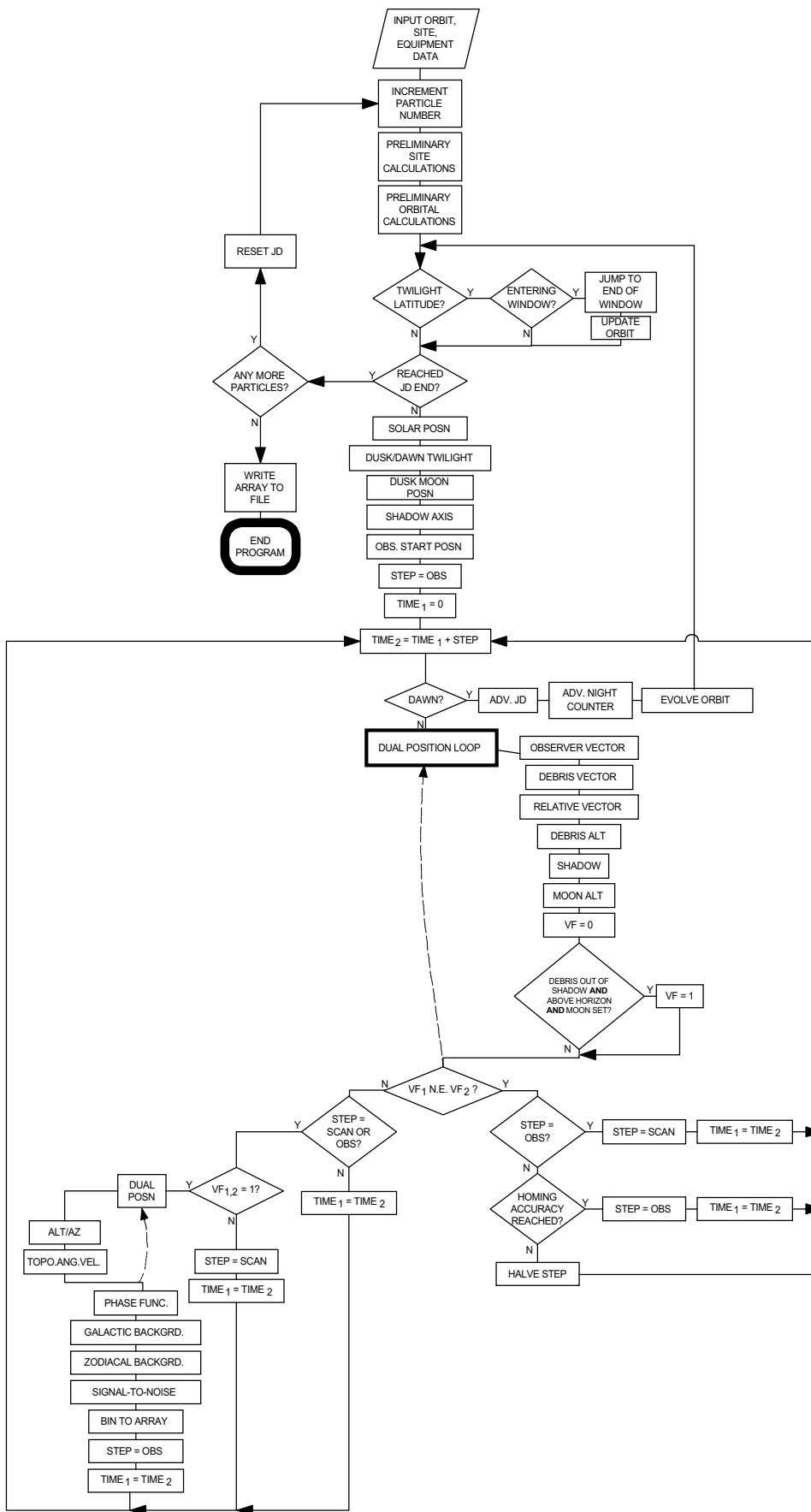


Figure 3.1: Basic flowchart of the SkyPlot program.

## 3.4 Program Execution - In Detail

### 3.4.1 Abort Scenarios

Next in the program's execution schedule is addressing the following situations that would lead to the debris particle never being detected, and thereby wasting execution time (if they are identified immediately then the program aborts with a diagnostic message).

#### 3.4.1.1 Geometric Effects

A low orbit with low inclination will not be visible to an observer at high latitudes at all. Consequently a debris particle in such an orbit will never be detected, and any attempt at running the SkyPlot program under these conditions would be a waste of time. The maximum possible latitude from which the debris orbit could be viewed irrespective of illumination or phase considerations is calculated by rotating the orbit in its orbit plane such that the apogee is at the greatest geocentric latitude possible in the hemisphere of the observatory and the line of sight from apogee to the Earth's surface can then be produced (Figure 3.2).

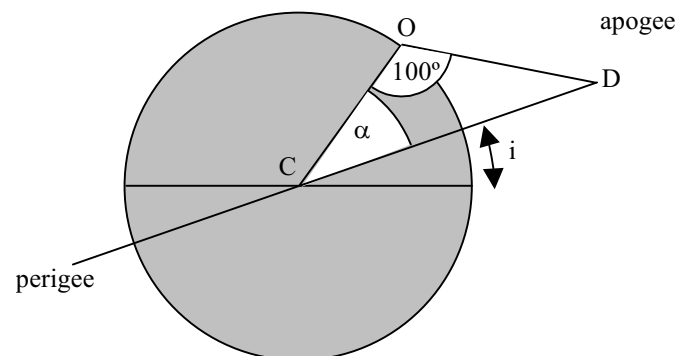


Figure 3.2: Calculating maximum latitude of observation. Debris at D, observer at O. Debris subtends angle of  $10^\circ$  to horizon.

The zenith distance for which this calculation is made is taken to be  $80^\circ$  due to excessive atmospheric extinction closer to the horizon (see later). This figure is optimistically the best possible case, since most telescopes would not be able to reach a zenith distance of  $80^\circ$ . From Figure 3.2 the maximum latitude can be calculated by:

$$L = 80^\circ - \sin^{-1}\left(\frac{r_e}{R} \sin 100^\circ\right) + i. \quad (3.1)$$

### 3.4.1.2 Twilight Latitudes

Observing sites close to the poles experience the “midnight sun” effect for some time around the summer solstice for their hemisphere. However, for observing faint objects, the Sun should not only be below the horizon, but at least  $18^\circ$  below the horizon (a solar zenith distance of  $108^\circ$ ) in order for the sky to be astronomically dark (Figure 3.3).

An observer close to the poles experiences therefore a “twilight window” of time during local summer in which observing is impractical because the sky is too bright. To avoid unnecessary execution through a period of many days when the debris is not visible the program skips this period, incrementing the parameters of the debris orbit by the appropriate amount.

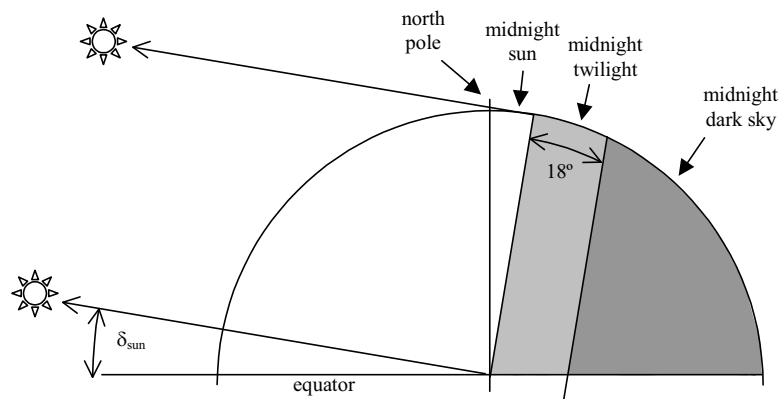


Figure 3.3: Relation between twilight types and position along solar meridian.

#### 3.4.1.2.1 Twilight Window Calculation

At the beginning of the program, the start and finish years and the site latitude are used to calculate in advance the Julian dates of the start ( $S_n$ ) and finish ( $F_n$ ) of each window to occur in every year  $n$  in the sequence. These dates are stored in an array and are compared with the current Julian date at the start of every night’s observing in the simulation. If the current Julian date falls within any twilight window (i.e. if  $S_n < [\text{current Julian date}] < F_n$ ), the current Julian date jumps to the day after  $F_n$  of that year.

These calculations are performed by first determining the phase angle of the

astronomical twilight terminator as measured from the subsolar point. We remember that the astronomical twilight terminator is  $18^\circ$  further from the subsolar point than the sunset terminator (Figure 3.3), the exact phase angle of which is calculated below.

With reference to Figure 3.4, the phase angle of the sunset terminator is computed using similar triangles (assuming the Sun and Earth are perfect spheres) - the horizontal axis of the figure is the heliocentric radius vector of the Earth.

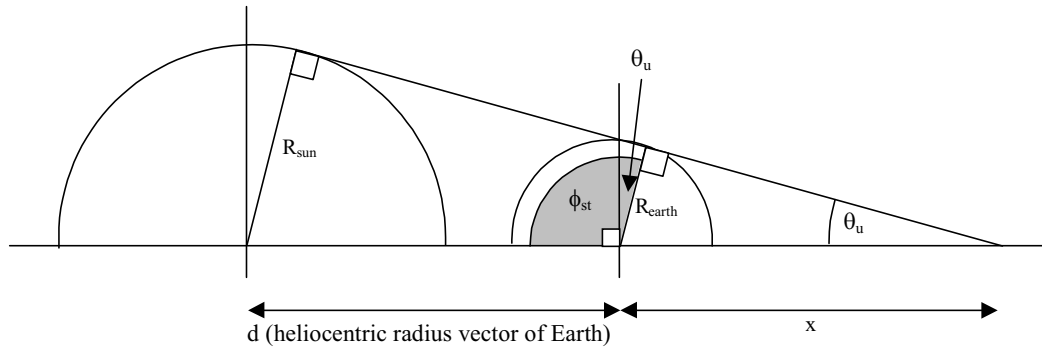


Figure 3.4: Relation between phase angle of sunset terminator and the half-angle of the umbral cone. Angles  $\theta_u$  and  $\theta_{st}$  explained in the text.

The half angle of the umbra cone is therefore given by:

$$\theta_u = \sin^{-1} \left[ \frac{R_{\text{sun}} - R_{\text{earth}}}{d} \right]. \quad (3.2)$$

The sunset terminator phase angle  $\phi_{st}$  is therefore:

$$\phi_{st} = \frac{\pi}{2} + \theta_u = 90.2641^\circ, \quad (3.3)$$

using  $R_{\text{sun}} = 6.9599 \times 10^8$  m,  $R_{\text{earth}} = 6.3780 \times 10^6$  m,  $d = 1 \text{ AU} = 1.4960 \times 10^{11}$  m (Allen, 1973). Therefore, the astronomical twilight terminator phase angle  $\phi_{tw}$  is given by:

$$\phi_{tw} = \phi_{st} + 18^\circ = 108.2641^\circ. \quad (3.4)$$

The relationship between  $\phi_{tw}$  and latitude depends on the declination of the Sun, which varies with the time of year. We define the ‘‘astronomical twilight supplementary latitude’’  $L_{ats}$  as the angle between the equator and the astronomical twilight terminator, measured along the meridian passing through the subsolar point and Earth’s axis, (Figure 3.5) as:

$$L_{ats} = \phi_{at} + \delta_{\text{sun}}. \quad (3.5)$$

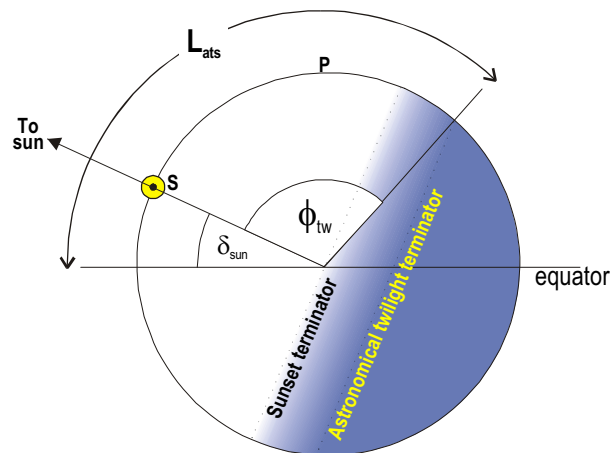


Figure 3.5: Derivation of astronomical twilight supplementary latitude  $L_{ats}$ . The plane of the paper is that containing the Earth's polar axis and the Sun. The north pole is situated at P, the subsolar point at S. The astronomical twilight terminator is always at a geocentric angle of  $\phi_{tw} = 108.2641^\circ$  from the subsolar point, whatever the sun's declination  $\delta_{sun}$ .  $L_{ats}$  is measured however from the equator on the sunward side of the Earth, so in the case depicted here of northern hemisphere summer,  $L_{ats}$  has a value of  $\delta_{sun}$  plus  $\phi_{tw} = 23.5^\circ + 108.2641^\circ = 131.7641^\circ$ .

Viewing Figure 3.5 from above the north pole gives Figure 3.6 (as an aid to understanding Figure 3.7; see next paragraph). An observer at e.g.  $70^\circ\text{N}$  would therefore transcribe a circular path ABA about the north pole P due to the Earth's diurnal rotation. The point at which the sky could not get any darker for the observer is at B, at the greatest phase angle from the sun. Analysis of the sky brightness at this point only determines whether the sky is dark enough for observing at all; at other points on the observer's path the sky would be brighter anyway. It can be seen that the point D must be much closer to the pole than B for the observer to experience a truly dark sky for any appreciable length of time (in the example shown of summer solstice, the sun is above the horizon).

Plotting  $L_{ats}$  for points A, B, C & D in Figure 3.6 against day number gives Figure 3.7. Points A & B of the observer's path are shown as horizontal lines as their position does not change with respect to the equatorial point E in Figure 3.6, while points C & D exhibit sinusoidal motion. It can be seen that between day numbers 85 and 261 for each year the night sky is too bright for observing – the sky brightness is at least above the threshold of astronomical twilight (and between approximate day numbers 140-195 the sun is above the horizon as well; though this is not indicated on the graph for clarity). Program execution should therefore avoid day numbers 85 to 261 inclusive for that year. An observing run of more than one year duration would produce a timeline of observing and twilight windows looking schematically like Figure 3.8.

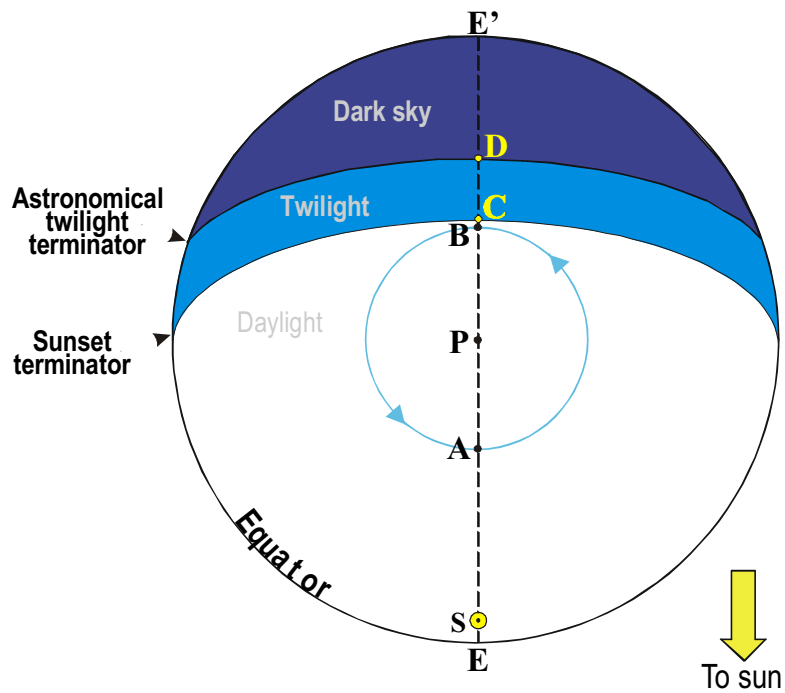


Figure 3.6: View of the Earth at northern hemisphere summer solstice from above the North Pole. Positions marked are subsolar point (S), north pole (P), diurnal path of observer at 70°N (ABA), intersections of Sun-Earth-Celestial Pole plane with sunset and astronomical twilight terminators (C & D respectively).

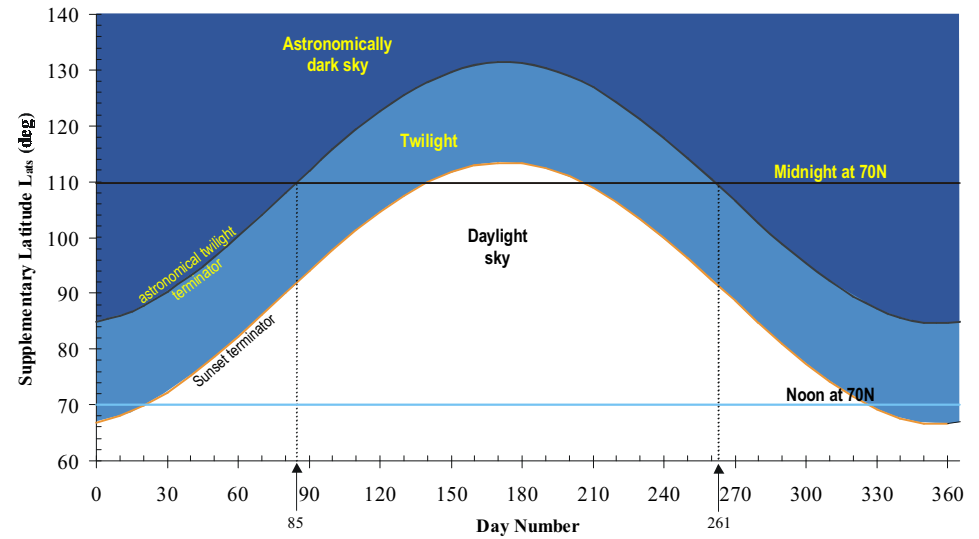


Figure 3.7: Graph of supplementary astronomical twilight latitude  $L_{ats}$  variation throughout the year. Sunset supplementary latitude curve also shown. A point on the graph effectively shows the value of the arc ED in Figure 3.6. Solid black line at  $L_{ats} = 110^\circ$  denotes supplementary latitude of observer at midnight at 70° N. It can be seen that between day numbers 85 and 261 the sky brightness never becomes astronomically dark.

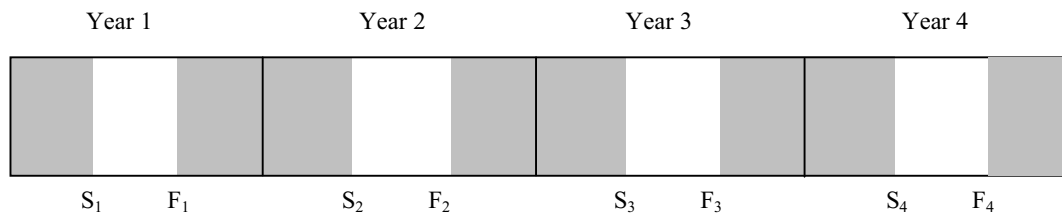


Figure 3.8: Qualitative illustration of the concept of twilight windows along an observing timeline, where the brightness of the sky never falls below that of astronomical twilight. The black rectangles denote calendar years, within which the shaded areas represent times when the night sky is dark enough for observing, and the white areas are the times (during four calendar years in the northern hemisphere summer in this example) when the sky is too bright. The start/finish dates of each year's twilight window are shown as the dates S,F.

The entire Polar Illumination coding strategy was introduced out of necessity because of the SkyPlot algorithm's initial daytime avoidance code calculating the time of local sunset/sunrise for each day in the observing run and "jumping" its time increments from one sunrise to the next sunset. It was easier to work around this algorithm rather than change it, hence the polar illumination avoidance algorithm presented in this section. It was also too complex to include the 24-h astronomically dark sky effect that would be found within  $5.2^\circ$  of the poles in local winter (consider an observer at  $90^\circ\text{N}$  in Figure 3.7 for example); hence the SkyPlot program is suitable only for latitudes within  $\pm 84.8^\circ$ . This however amounts to more than 99% of the Earth's surface, and so the loss of coverage is negligible.

### 3.5 Summary

This chapter described the concept of the Alt-Az Pattern of detectability and presented an overview of the generating program "SkyPlot" in basic terms. The next chapter looks at each aspect of the program's astronomical and physical considerations in detail.